

SPECTRAL DISCRIMINATION OF AVALANCHE DEPOSITS

D. Treichler *, Y. Bühler, A. Hueni, M. Kneubühler, K.I. Itten

Remote Sensing Laboratories (RSL), University of Zürich,
Winterthurerstrasse 190, 8057 Zürich, Switzerland –
(dtreichl, ybuehler, ahueni, kneub, itten)@geo.uzh.ch

KEY WORDS: Avalanche detection, field spectroradiometer, imaging spectrometry, absorption feature

ABSTRACT

In the past, remote sensing of snow and ice has mainly been undertaken to determine the extent of snow-covered areas and to investigate snow properties such as grain size or contaminants. Meanwhile, the research on the spatial distribution of avalanches has remained marginal. A method for automatic classification of avalanches in satellite or aerial imagery would greatly enlarge the possibilities of avalanche modelling and forecast evaluation.

Snow avalanches originate from mountain slopes further uphill where a different and usually colder temperature regime prevails. During the descent of an avalanche, different layers are mixed, the snow agglomerates and occasionally soil and vegetation material is accumulated. Avalanche deposits differ from undisturbed snow by their densities, grain sizes and contaminations by impurities. In this study, more than 400 spectra of nine avalanche deposits and adjacent undisturbed snow cover have been measured in the Davos region in the Swiss Alps in January and April 2008 using an ASD Field Spectroradiometer. Normalisation of the spectra was required due to high variance in reflectance values caused by shadow effects and different avalanche parameters. Continuum removal of absorption features highlighted significant relative differences in reflectance and allowed for local separation between snow and avalanche spectra. Three groups of dirty, wet and recent deposits could be distinguished. The comparability between the deposits is low due to high variance of avalanche spectra; nevertheless an overall classification accuracy of 86% could be reached using area and depth of specific absorption features.

1. INTRODUCTION

An avalanche is a rapid downward movement of snow driven by gravitation and can be triggered both by natural cause and by human activity. Avalanches occur in the form of loose powder snow clouds, compact slab avalanches, wet slush avalanches or mixed forms and involve high velocities and forces. Avalanche paths consist of starting zone, track and runout (deposition zone). Due to different microclimates, the snow properties of starting and deposition zone differ (Schweizer et al., 2008). During the descent, different layers are mixed, the snow agglomerates and occasionally soil and vegetation material is accumulated. The deposited avalanche snow and the adjacent undisturbed snow cover are expected to differ in density, grain size and contaminations by impurities.

Avalanches are a danger not only to villages, traffic lines, energy plants and lines, but also to backcountry and off-slope skiers: 25 persons die every year due to avalanches in Switzerland (Harvey and Zweifel, 2008). Structural standards and measures such as avalanche protection works help to reduce the risk of avalanche hazards. In the future, avalanche activity is likely to increase in higher elevated areas due to an increase of precipitation in the Alps in winter (OcCC/ProClim-, 2007). At the same time backcountry and off-slope skiing became more popular. For the safety of winter tourists, precise and reliable avalanche forecasting is essential.

Mapping and modelling of avalanches is currently based on observations of recent and past avalanche events (McClung and Schaerer, 2006, Purves et al., 2003, Schweizer and Föhn, 1996). For monitoring purposes and to enhance forecasting accuracy, it would be useful to automatically classify avalanches in satellite or aerial imagery (Bühler et al., 2009). While the spectral properties of snow and ice are well studied (Warren and Wiscombe, 1980; Wiscombe and Warren, 1980; Warren, 1982; Dozier and Painter, 2004; Gupta et al., 2005), the research on avalanches using remote sensing techniques has remained marginal. Sharma et al. (2004) found that the fusion of optical and microwave data allows to detect significant changes in snow characteristics that are accompanied by changes in avalanche activity. Bühler et al. (2009) used directional, textural and spectral properties to automatically classify avalanche deposits in high resolution multispectral imagery. However, no attempt has been undertaken to determine whether avalanche deposits and undisturbed snow can be discriminated using imaging spectroscopy data. In this study, the spectral properties of avalanche deposits and adjacent undisturbed snow are analysed to identify spectral features where discrimination is possible and to assess the influences of snow properties, impurities, measurement conditions and avalanche types.

2. STUDY AREA AND DATA COLLECTION

Spectroradiometry measurements of nine avalanche deposits and adjacent undisturbed snow cover were taken using an ASD Field Spectrometer. 421 nearly continuous curves with

* Corresponding author.

ID	Date of observation	Slope aspect	Altitude [m]	Avalanche type
1	26.04. 12:00	NE	2200	Slab avalanche, slightly snow-covered, 3 days old
2	26.04. 14:30	E	2300	Powder avalanche, slightly snow-covered, 2 days old
3	27.04. 10:00	N	1580	Slab avalanche, contaminations, wet after rainfall, 4 d old
4	27.04. 12:15	NE	1820	Slab avalanche, contaminations, wet after rainfall, 4 d old
5	27.04. 12:50	NE	1860	Slab avalanche, contaminations, wet after rainfall, 4 d old
6	27.04. 14:25	NE	1690	Slab avalanche, very dirty, wet after rainfall, 4 days old
7	27.04. 15:45	SE	1630	Slab avalanche, clean to dirty, big block deposits, 5 days old
8	20.01. 12:40	SW	2490	Slab avalanche, dry and clean snow, 1 day old
9	20.01. 14:30	NW	2240	Slab avalanche, dry and clean snow, from the same day

Table 1. Avalanche parameters.

a spectral range of 350-2500 nm were collected in January and April 2008 in the area of Davos, Switzerland. The town is located at 1560 m asl in the south-eastern part of the Swiss Alps and surrounded by peaks mostly between 2500 and 2800 m asl. The backcountry is easily accessible due to the existing ski resort infrastructure. The selected avalanche deposits comprise varying types of avalanches, snow properties, amounts of impurities, slope aspects and altitudes. Some avalanche deposits are slightly snow-covered or wet after rainfall, as summarised in table 1.

3. METHODS

3.1 Preprocessing and statistical approach

To remove noise, a Savitzky-Golay smoothing filter (Savitzky and Golay, 1964) was applied to the spectra. The filter removes noise while preserving the original shape of the curve. The signal is highly noisy in the water absorption bands at 1350-1400, 1800-1950 and 2350-2500 nm. These wavelengths were excluded from statistical analysis and linearly interpolated for the following processing steps to avoid discontinuities in the spectral curves.

For all nine sites, mean and variance of the snow and avalanche deposit spectra were calculated to characterise the avalanche deposits and describe the differences between the sites. Separability between the avalanche and adjacent snow spectra was estimated by performing a Wilcoxon rank sum test of differences between the groups per study site.

3.2 Continuum removal

The shape of the curves can not be compared using the absolute values due to high variance in reflectance values. Continuum removal highlights significant relative differences in reflectance as it relates the spectra to its continuum, usually represented by a convex hull. This results in normalisation of the reflectance to values between 0 and 1 (Eq. 1). A value of 0 indicates that the the reflectance of the spectrum R_s is zero and maximally different to the

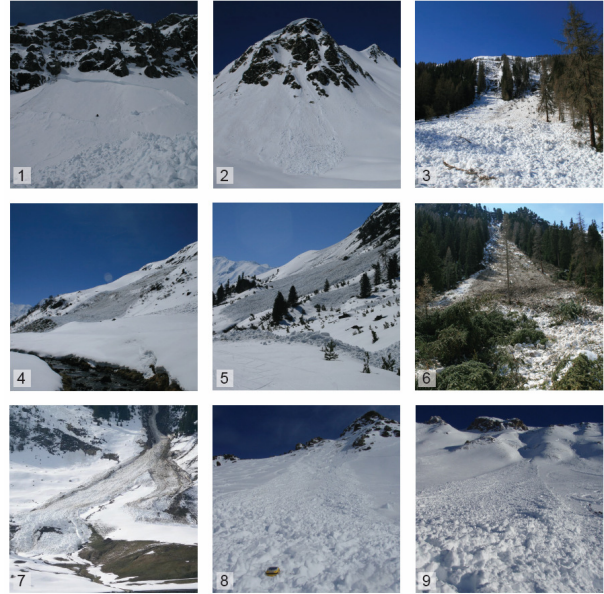


Figure 1. Avalanche deposits, ID 1-9

corresponding continuum R_c . Where the absolute reflectance matches the value of the continuum, the normalised value becomes 1 (Clark and Roush, 1984).

$$C = \frac{R_c - R_s}{R_c} \quad (1)$$

Since the general shape of snow spectral curves is concave, a convex hull around the whole curve would not touch the spectrum between about 700 and 2250 nm. To separate and emphasize the multiple absorption features, the hull was forced to touch the spectrum at local maxima. The continuum was represented by straight line segments between these touch points and made to follow the spectral curve where the curve shape is convex (Fig. 2).

3.3 Feature area and depth

As stated by Wiscombe and Warren (1980), snow albedo in the NIR is highly dependent on grain size, which can be

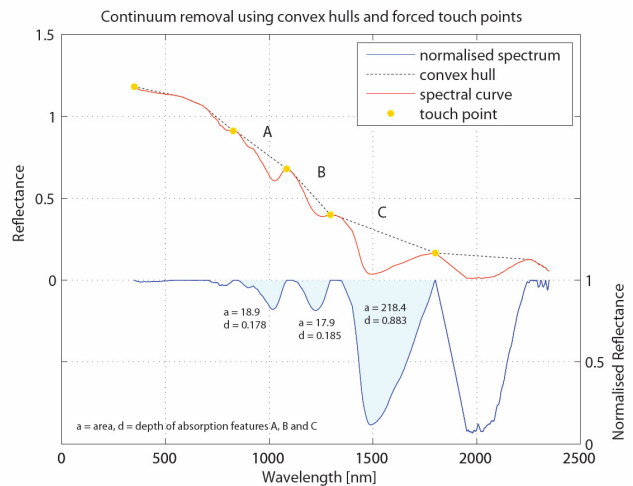


Figure 2. Feature area and depth using continuum removal

observed in the depth and shape of absorption features of the spectra. Consequently, the agglomeration of avalanche deposit snow or the most probably different grain size between avalanche deposits and adjacent undisturbed snow might be used for classification purposes. Feature depth d and area a were retrieved from the continuum removed spectra for three absorption features centred at 1.02 (A), 1.22 (B) and 1.5 μm (C) approximately (Fig. 2, Eq. 2). The absorption feature centred at 2 μm was not considered due to high noise in the data. The metrics d and a are calculated as follows:

$$d = 1 - Rc_{\min} \quad (2)$$

$$a = \int_{\lambda} 1 - Rc$$

The use of absorption feature area reduces the uncertainty of the retrieved value, as fluctuations caused by sensor noise should average out (Nolin and Dozier, 2000). On the other hand, the wideness of the absorption feature highly affects the feature area and reduces the influence of feature depth. To take into account this dependency, both, area and depth were calculated.

3.4 Discrimination methods

To quantify the separability between avalanche deposits and adjacent undisturbed snow, feature area and depth values were used to calculate Bhattacharyya (BH) (Bhattacharyya, 1843) and Jeffries-Matusita (JM) distances. The JM distance between a pair of probability functions is the measure of the average distance between the two class density functions (Richards, 1993). For normally distributed classes, this distance becomes the BH distance (Richards, 1993). A large BH distance value indicates a better separability of the classes. A JM distance of 2 indicates maximal separability.

Using half of the samples of each group as training samples, a discriminant analysis of the remaining spectra with a) linear and b) quadratic decision boundary was performed using the

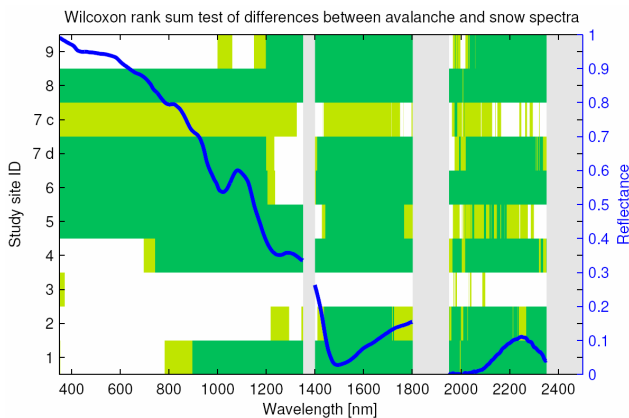


Figure 3. Separability per wavelength using Wilcoxon rank sum test. For site 7, dirty (7d) and clean (7c) parts are treated separately. White: no difference, light grey: filtered water absorption bands, green: separation possible – significance level: 95% light green, 99.9 % dark green. The snow reflectance curve is displayed to relate the separability to typical spectral features.

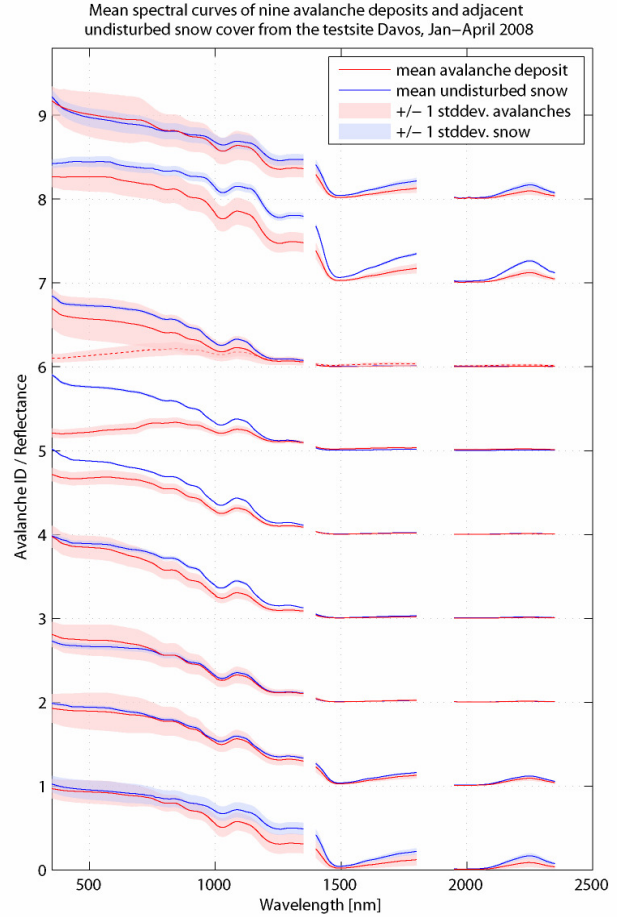


Figure 4. Means and standard deviations of the spectra per set site.

feature area and depth values. This was done for all sites separately as well as for comparing all snow spectra to all avalanche deposits spectra.

4. RESULTS

4.1 Results of the statistical analysis

The separability test indicates a difference between the snow and avalanche deposit spectra in the NIR (Fig. 3). In the spectral range between 1400 and 1800 nm, for all sites except 3 and 7, the test is highly significant. In the VIS only the dirty deposits 6 and 7 d and sites 5 and 8 are statistically separable.

The visual analysis of means and variances of the spectra show that avalanche deposits have a generally lower mean reflectance than undisturbed snow (Fig. 4). The variance of avalanche spectra is large especially in the VIS and the NIR while the snow spectra show a low variance over the whole spectrum. The reflectance of the dirty deposits 6 and 7 is noticeably reduced in the VIS due to the light-absorbing impurities (Warren and Wiscombe, 1980). The deposits and adjacent snow of site 3, 4, 5, 6 and 7 that are wet after rainfall have a reduced mean reflectance in the NIR compared to sites 1, 2, 8 and 9. For these recent or slightly snow-covered deposits, mean reflectance of undisturbed snow is higher in the NIR than for avalanche deposit snow.

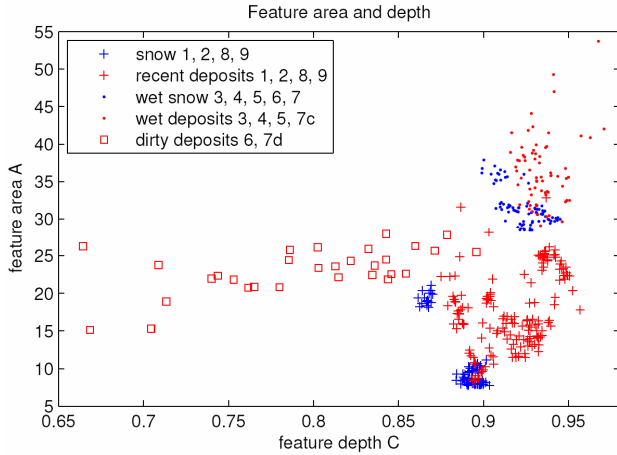


Figure 5. Wet, recent and dirty deposits and adjacent undisturbed snow displayed using the most distinguishing absorption features: Feature area A ($1.02 \mu\text{m}$) and feature depth C ($1.5 \mu\text{m}$).

4.2 Continuum removed data

Continuum removal accentuates the different behaviour of avalanche deposits and undisturbed snow in the NIR where the reflectance is low and divergences are difficult to identify visually. Differences in feature areas and depths can be observed in all three absorption features. For sites 1, 6, 7d, 8 and 9, the Kruskal-Wallis test of variance states highly significant differences in feature areas and depths for all three absorption features (Tbl. 2). For the feature depth at $1.5 \mu\text{m}$ approximately, the test results in statistically significant differences for all sites. Feature depth for this feature is bigger for avalanche deposits spectra than for snow except for dirty deposits where the feature depth of avalanche spectra is remarkably reduced compared to snow feature depth.

ID	$1.02 \mu\text{m}$		$1.22 \mu\text{m}$		$1.5 \mu\text{m}$	
	area	depth	area	depth	area	depth
1	0	0	0	0	0	0.015
2	59.9	76.3	70.6	47.4	0.001	0
3	0	0.094	5.67	4.43	0.752	0
4	0	0	0.055	0	44.8	0.003
5	0.003	0.042	23.5	47.1	1.43	0.690
6	0	0.001	0	0	0	0
7 _{dirty}	0	0	0	0	0	0
7 _{clean}	30.9	65.8	96.5	79.1	42.5	0.001
8	0	0	0	0	0	0
9	0	0	0	0	0	0
all	6.64	4.87	58.6	87.7	13.2	0

Table 2. Kruskal-Wallis test of variance for differences between the medians of snow and avalanche deposits spectra. The displayed values show the probability in percent for equality of the two groups. Low values indicate high separability, values smaller than 0.0005 % are displayed as zero.

ID	JM	BH	Linear		Quadratic	
			OA %	κ	OA %	κ
1	1.98	4.48	92.0	0.77	94	0.81
2	1.98	4.71	93.8	0.88	100	1
3	2	8.31	95	0.90	75	0.42
4	1.99	4.93	94.7	0.90	94.7	0.90
5	1.99	5.62	100	1	87.5	0.75
6	2	9.37	100	1	100	1
7 _{dirty}	2	11.11	100	1	100	1
7 _{clean}	1.94	3.59	90.5	0.81	100	1
8	2	6.10	100	1	100	1
9	2	15.60	100	1	100	1
all	1.51	1.40	80	0.59	86.2	0.72

Table 3. Jeffries-Matusita and Bhattacharyya distances, overall accuracy (OA) and κ -coefficient of linear and quadratic classification.

JM- and BH-distances are highest for sites 3, 6, 7d, 8 and 9 but indicate a good local separability in general, whereas the distance between all avalanche spectra and all snow spectra is low (Tbl. 3). Nevertheless, a classification using feature depth and area of all three absorption features results in overall accuracies of 80 and 86.2 percent and κ -coefficients of 0.59 and 0.72 for linear and quadratic classifiers respectively.

5. CONCLUSION

The comparability between different avalanche types and different sites is poor due to high variance of avalanche deposit spectra. The separability tests indicate higher separability in the NIR than in the VIS. When looking at means and variances, three groups of avalanche spectra can be distinguished: Dirty deposits with remarkably reduced reflectance in the VIS, wet snow and avalanche deposits with a reflectance of nearly zero in the spectral range between 1.4 and $2.5 \mu\text{m}$, and recent or slightly snow-covered deposits. For latter sites, the mean reflectance of undisturbed snow is higher in the NIR than for avalanche deposit snow.

In the normalised data, significant relative differences in shape and depth of absorption features are visible: Avalanche and snow spectra behave differently in absorption features. Statistically significant differences in depth of the absorption feature centred at $1.5 \mu\text{m}$ can be observed for all sites: The feature depth of avalanche deposits spectra is higher for all sites except for the very dirty deposits, where the feature depth of avalanche spectra is much lower than for snow spectra. This difference is highly significant even when comparing all avalanche spectra to all snow spectra. Using the area and depth values of all three absorption features, classification is possible with overall accuracies of 90-100% for each site separately and 86.2 % for all spectra together.

Normalisation of spectroradiometer data allows for discrimination of avalanche deposits and adjacent undisturbed snow cover. Significant differences in absorption features are

detectable. However, these differences are small and vary highly with avalanche types, snow properties and measurement conditions. Further research involving more spectral data and various avalanche types is needed to assess if the reported differences are apparent in high resolution airborne or satellite spectroscopy images.

REFERENCES

- Bhattacharyya, A. (1943). On a measure of divergence between two statistical populations defined by probability distributions. *Bulletin of Calcutta Maths Society*, vol. 35, pp. 99–110.
- Bühler, Y., Hüni, A., Christen, M., Meister, R. and Kellenberger, T. (in press). Automated detection and mapping of avalanche deposits using airborne optical remote sensing data. *Cold Regions Science and Technology*, accepted 13 February 2009.
- Clark, R.N. and Roush, T.L. (1984). Reflectance Spectroscopy: Quantitative Analysis Techniques for Remote Sensing Applications. *Journal of Geophysical Research*, vol. 89 (B7), pp. 6329–6340.
- Dozier, J. and Painter, T.H. (2004). Multispectral and Hyperspectral remote sensing of alpine snow properties. *Annual Review of Earth and Planetary Sciences*, vol. 32, pp. 465–494.
- Gupta, R.P., Haritashya, U.K. and Singh, P. (2005). Mapping dry/wet snow cover in the Indian Himalayas using IRS multispectral imagery. *Remote Sensing of Environment*, vol. 97 (4), pp. 458–469.
- Harvey, St. and Zweifel, B. (2008). New trends of recreational avalanche accidents in Switzerland. *International Snow Science Workshop*, Whistler, BC, Canada, September 21–27 2008. WSL Swiss Federal Institute for Snow and Avalanche Research SLF.
- McClung, D.M. and Schaerer, P. (2006). *The Avalanche Handbook*. The Mountaineers Books, Seattle, 342 pp.
- Nolin, A.W. and Dozier, J. (2000). A Hyperspectral Method for Remotely Sensing the Grain Size of Snow. *Remote Sensing of Environment*, vol. 74 (2), pp. 207–216.
- OcCC/ProClim- (2007). *Klimaänderung und die Schweiz 2050 – Erwartete Auswirkungen auf Umwelt, Gesellschaft und Wirtschaft*. OcCC/ProClim-, Bern, Switzerland.
- Purves, R.S., Morrison, K.W., Moss, G. and Wright, D.S.B. (2003). Nearest neighbours for avalanche forecasting in Scotland – development, verification and optimisation of a model. *Cold Regions Science and Technology*, vol. 37 (3), pp. 343–355.
- Richards, J.A. (1993). *Remote Sensing Digital Image Analysis*. Springer, Berlin.
- Savitzky, A. and Golay, M.J.E. (1964). Smoothing and Differentiation of Data by Simplified Least Squares Procedures. *Analytical Chemistry*, vol. 36 (8), pp. 1627–1639.
- Schweizer, J. and Föhn, P.M.B. (1996). Avalanche forecasting – an expert system approach. *Journal of Glaciology*, vol. 42 (141), pp. 318–332.
- Schweizer, J., Kronholm, K., Jamieson, J.B. and Birkeland, K.W. (2008). Review of spatial variability of snowpack properties and its importance for avalanche formation. *Cold Regions Science and Technology*, vol. 51 (2-3), pp. 253–272.
- Sharma, S., Mathur, P. and Snehmami (2004). Change detection analysis of avalanche snow in Himalayan region using near infrared and active microwave images. *Advances in Space Research*, Vol. 33, 259–267.
- Warren, S. (1982). Optical Properties of Snow. *Reviews of Geophysics and Space Physics*, vol. 20, pp. 67–89.
- Wiscombe, W.J. and Warren, S.G. (1980). A Model for the Spectral Albedo of Snow. I: Pure Snow. *Journal of the Atmospheric Sciences*, vol. 37 (12), pp. 2712–2733.
- Warren, S.G., and Wiscombe, W.J. (1980). A Model for the Spectral Albedo of Snow. II: Snow containing Atmospheric Aerosols. *Journal of the Atmospheric Sciences*, vol. 37 (12), pp. 2734–2745.